7. STRUCTURE OF NUCLEI

In section 2 we looked at some of the phenomena of nuclear physics. In this section we return to nuclear physics and discuss some theoretical models that tell us more about the structure of nuclei.

7.1 Fermi Gas Model

In this model, the protons and neutrons that make up the nucleus are assumed to comprise two independent systems of nucleons, each freely moving inside the nuclear volume subject to the constraints of the Pauli principle. The potential felt by every nucleon is the superposition of the potentials due to all the other nucleons. In the case of neutrons this is assumed to be a finite-depth square well; for protons, the Coulomb potential modifies this. A sketch of the potential wells in both cases is shown in Fig.7.1.

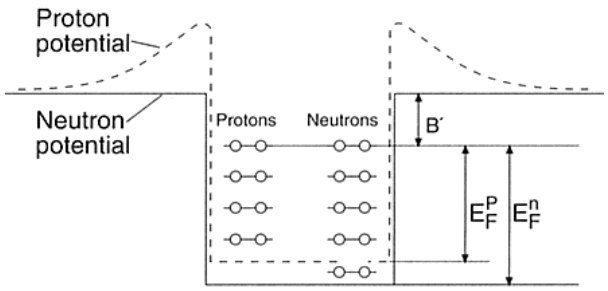

Fig.7.1 Proton and neutron potentials and states in the Fermi gas model

For a given ground state nucleus, the energy levels will fill up from the bottom of the well. The energy of the highest level that is completely filled is called the *Fermi level* of energy E_F and has a momentum $p_F = \sqrt{2ME_F}$, where M is the mass of the nucleon. Within the volume V, the number of states with a momentum between p and $p + dp$ is given by

$$n(p)dp = dn = \frac{4\pi V}{(2\pi\hbar)^3} p^2 dp$$

[**Note:** This is the so-called *density of states factor* and may be found as follows. Firstly, solve the Schrödinger equation for a free particle in a box of side L, with volume $V = L^3$, subject to the boundary conditions that the wave function vanishes on all faces of the cube. This restricts the allowed wave numbers k to the values

$$\mathbf{k} = \left(\frac{\pi}{L}n_1, \frac{\pi}{L}n_2, \frac{\pi}{L}n_3\right)$$

where n_1 etc are integers. Plotting these in a three dimensional grid gives the number of modes of standing waves with wave number **k** having magnitude in the range k to $k + dk$ as

$$f(k)\,dk = \frac{V k^2}{2\pi^2} dk$$

Finally, using $\mathbf{p} = \hbar\mathbf{k}$, gives the result above.] Since every state can contain two fermions of the same species, we can have (using $n = 2\int_0^{p_F} dn$)

$$N = \frac{V(p_F^n)^3}{3\pi^2\hbar^3} \quad \text{and} \quad Z = \frac{V(p_F^p)^3}{3\pi^2\hbar^3}$$

neutrons and protons, respectively. With a nuclear volume

$$V = \frac{4}{3}\pi R^3 = \frac{4}{3}\pi R_0^3 A$$

where experimentally $R_0 = 1.21\text{fm}$ (as we have seen from electron scattering experiments discussed in Section 2) and assuming the depths of the neutron and proton wells to be the same, we find for a nucleus with $Z = N = A/2$, the Fermi momentum

$$p_F = p_F^n = p_F^p = \frac{\hbar}{R_0}\left(\frac{9\pi}{8}\right)^{1/3} \approx 250\,\text{MeV/c}$$

Thus the nucleons move freely within the nucleus with large momenta.

The Fermi energy is

$$E_F = \frac{p_F^2}{2M} \approx 33\text{MeV}$$

The difference B' between the top of the well and the Fermi level is constant for most nuclei and is just the average binding energy per nucleon $B/A = 7 - 8\text{MeV}$. The depth of the potential and the Fermi energy are to a good approximation independent of the mass number A:

$$V_0 = E_F + B' \approx 40\text{MeV}.$$

Heavy nuclei generally have a surplus of neutrons. Since the Fermi levels of the protons and neutrons in a stable nucleus have to be equal (otherwise the nucleus can become more stable by β-decay) this implies that the depth of the potential well for the neutron gas has to be deeper than for the proton gas, as shown in Fig.7.1. Protons are therefore on average less tightly bound in nuclei than are neutrons.

We can use the Fermi gas model to give a theoretical expression for some of the dependence of the binding energy on the surplus of neutrons, as follows.

First we define the average kinetic energy per nucleon

$$\langle E_{kin}\rangle = \frac{\int_0^{p_F} E_{kin} p^2\,dp}{\int_0^{p_F} p^2\,dp} = \frac{3}{5}\frac{p_F^2}{2M} \approx 20\text{MeV}$$

The total kinetic energy of the nucleus (which is a good approximation to B') is then

$$E_{kin}(N,Z) = N\langle E_n\rangle + Z\langle E_p\rangle = \frac{3}{10M}\left[N(p_F^n)^2 + Z(p_F^p)^2\right]$$

which may be re-expressed as

$$E_{kin}(N,Z) = \frac{3}{10M}\frac{\hbar^2}{R_0^2}\left(\frac{9\pi}{4}\right)^{2/3}\left[\frac{N^{5/3}+Z^{5/3}}{A^{2/3}}\right]$$

where again we have taken the radii of the proton and neutron wells to be equal. This expression is for fixed A but varying N and has a minimum at $N = Z$. Hence the binding energy gets smaller for $N \neq Z$. If we set $N = (A+\Delta)/2$, $Z = (A-\Delta)/2$ and expand this expression in a power series in Δ/A, where $\Delta \equiv N - Z$, we obtain

$$E_{kin}(N,Z) = \frac{3}{10M}\frac{\hbar^2}{R_0^2}\left(\frac{9\pi}{8}\right)^{2/3}\left[A + \frac{5}{9}\frac{(N-Z)^2}{A} + ...\right]$$

which gives the dependence on the neutron surplus. The first term contributes to the volume term in the semi-empirical mass formula (SEMF), while the second describes the correction that results from having $N \neq Z$. This is the asymmetry energy we have met before and grows as the square of the neutron surplus. In practice, to reproduce the actual term in the SEMF accurately we would have to take into account the change in the potential for $N \neq Z$.

7.2 Shell Model

(a) Basic ideas

This model is based on the analogous model for the orbital structure of atomic electrons in atoms. It some areas it gives more detailed predictions than the Fermi gas model. Firstly, we recap the main features of the atomic case.

The binding energy of electrons in atoms is due primarily to the central Coulomb potential. This is a complicated problem to solve in general because in a multi-electron atom we have to take account of not only the Coulomb field of the nucleus, but also the fields of all the other electrons. Analytic solutions are not usually possible. However, many of the general features of the simplest case of hydrogen carry over to more complicated cases, so it is worth recalling these. Atomic energy levels are characterised by a quantum number $n = 1, 2, 3, 4, ...$

In atomic physics, n is called the principal quantum number and is defined so that it determines the energy of the system. In nuclear physics we are not dealing with the same simple coulomb potential, so it would be better to call n the *radial node quantum number*, as it still determines the form of the radial part of the wavefunction. For any n there are energy-degenerate levels with orbital angular momentum quantum numbers given by

$$\ell = 0,1,2,3,....,(n-1)$$

(this restriction follows from the form of the Coulomb potential) and for any value of ℓ there are $(2\ell+1)$ sub-states with different values of the projection of orbital angular momentum along any chosen axis (the magnetic quantum number)

$$m_\ell = -\ell, -\ell+1, .., 0, 1, ..., \ell-1, \ell$$

Due to the rotational symmetry of the Coulomb potential, all such sub-states will be degenerate in energy. Furthermore, since electrons have spin–1/2, each of the states above can

be occupied by an electron with spin "up" or "down", corresponding to the spin-projection quantum number

$$m_s = \pm 1/2$$

Again, both these states will have the same energy. So finally, any energy eigenstate in the hydrogen atom is labeled by the quantum numbers (n, ℓ, m_ℓ, m_s) and for any n, there will be n_d degenerate energy states, where

$$n_d = 2\sum_{\ell=0}^{n-1}(2\ell+1) = 2n^2$$

This high degree of degeneracy can be broken if there is a preferred direction in space, such as that supplied by a magnetic field, in which case the energy levels could depend on m_ℓ and m_s. One such interaction is the spin-orbit coupling, which is the interaction between the magnetic moment of the electron (due to its spin) and the magnetic field due to the motion of the nucleus (in the electron rest frame). This leads to corrections to the energy levels called *fine structure*.

In atomic physics, the fine structure corrections are small (of order α^2) and so if we ignore them for the moment, in hydrogen we would have a system with electron orbits corresponding to shells of a given n, with each shell having degenerate sub-shells specified by the orbital angular momentum ℓ. Going beyond hydrogen, we can introduce the electron-electron Coulomb interaction. This introduces a splitting to any energy level n according to the ℓ value. The degeneracies in m_l and m_s are unchanged. It is straightforward to see that if a shell or sub-shell is filled, then we have

$$\sum m_s = 0 \quad \text{and} \quad \sum m_\ell = 0$$

i.e. there is a strong pairing effect for closed shells. In these cases it can be shown that the Pauli principle implies

$$\mathbf{L} = \mathbf{S} = \mathbf{0} \quad \text{and} \quad \mathbf{J} = \mathbf{L} + \mathbf{S} = \mathbf{0}$$

For any atom with a closed shell or a closed sub-shell structure, the electrons are paired off and thus no valence electrons are available. Such atoms are therefore chemically inert. It is straightforward to work out the atomic numbers at which this occurs. These are

$$Z = 2,10,18,36,54$$

For example, the inert gas argon $\mathrm{Ar}(Z=18)$ has closed shells corresponding to $n = 1,2$ and closed sub-shells corresponding to $n = 3$, $\ell = 0,1$. These values of Z are called the *magic numbers.*

(b) Nuclear magic numbers

In nuclear physics, there is also evidence for magic numbers, i.e. values of Z and N at which the binding is particularly strong. This can been seen from the B/A curve of Fig.7.2, where at certain values of N and Z the data lie above the SEMF. (The figure only shows results for even values of the mass number A).

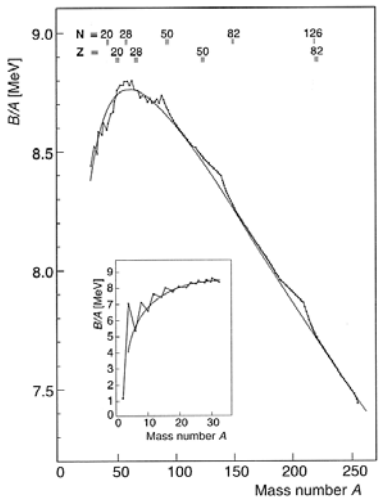

Fig.7.2 Binding energy per nucleon for even values of *A*. The solid curve is the SEMF.

The magic numbers are

$$N = 2,8,20,28,50,82,126$$
$$Z = 2,8,20,28,50,82$$

and correspond to one or more closed shells, plus 8 nucleons filling the *s* and *p* subshells of a nuclei with a particular value of *n.* Nuclei with both *N* and *Z* having one of these values are called *doubly magic*, and have even greater stability.

Shell structure is also suggested by a number of other phenomena. For example: "magic" nuclei have many more stable isotopes than other nuclei; they lack electric dipole moments, which means they are spherical; and neutron capture cross-sections show sharp drops compared to neighbouring nuclei. However, to proceed further we need to know something about the effective potential.

A simple Coulomb potential is clearly not appropriate and we need some form that describes the effective potential of all the other nucleons. Since the nuclear force is short-ranged we would expect the potential to follow the form of the density distribution of nucleons in the nucleus. So, for example, for very light nuclei this would be Gaussian and the potential could be an harmonic oscillator. For heavy nuclei, we have seen that the Fermi distribution fits the data and the corresponding potential is called the *Woods-Saxon* form

$$V_{central}(r) = \frac{-V_0}{1+e^{(r-R)/a}}$$

However, although these potentials can be shown to offer an explanation for the lowest magic numbers, they do not work for the higher ones. This is true of all purely central potentials.

The crucial step in understanding the origin of the magic numbers was taken in 1949 by Mayer and Jensen who suggested that by analogy with atomic physics there should also be a spin-orbit part, so that the total potential is

$$V_{tot} = V_{central}(r) + V_{\ell s}(r)\mathbf{L}.\mathbf{S}$$

where **L** and **S** are the orbital and spin angular momentum operators for a single nucleon and $V_{\ell s}(r)$ is an arbitrary function of the radial coordinate. This form for the total potential is the same as used in atomic physics except for the presence of the function $V_{\ell s}(r)$. Once we have coupling between **L** and **S** then m_ℓ and m_s are no longer "good" quantum numbers and we have to use eigenstates of the total angular momentum vector **J**, defined by $\mathbf{J} = \mathbf{L} + \mathbf{S}$. Squaring this, we have

$$\mathbf{J}^2 = \mathbf{L}^2 + \mathbf{S}^2 + 2\mathbf{L}.\mathbf{S}$$

i.e.

$$\mathbf{L}.\mathbf{S} = \tfrac{1}{2}\left(\mathbf{J}^2 - \mathbf{L}^2 - \mathbf{S}^2\right)$$

and hence the expectation value of $\mathbf{L}.\mathbf{S}$, which we write as $\langle \ell s \rangle$ is

$$\frac{\langle \ell s \rangle}{\hbar^2} = \frac{j(j+1) - \ell(\ell+1) - s(s+1)}{2} = \begin{cases} \ell/2 & \text{for } j = \ell + 1/2 \\ -(\ell+1)/2 & \text{for } j = \ell - 1/2 \end{cases}$$

(We are always dealing with a single nucleon, so that $s = 1/2$.) Thus the splitting between the two levels is

$$\Delta E_{ls} = \frac{2\ell+1}{2}\hbar^2 \langle V_{\ell s} \rangle$$

Experimentally, it is found that $V_{\ell s}(r)$ is negative, which means that the state with $j = \ell + 1/2$ will have a lower energy than the state with $j = \ell - 1/2$. This is opposite to the situation in atoms. Also, the splittings are substantial and increase linearly with ℓ. Hence for higher ℓ, level crossings can occur. Namely, for large ℓ, the splitting of any two neighbouring degenerate levels can shift the $j = \ell - 1/2$ state of the initial lower level to lie above the $j = \ell + 1/2$ level of the previously higher level.

An example of the resulting splittings up to the 1*G* state is shown in Fig.7.3, where the usual atomic spectroscopic notation has been used, i.e. levels are written $n\ell_j$ with $S, P, D, F, G, \ldots$ used for $\ell = 0, 1, 2, 3, 4, \ldots$ In this case a simple finite square well has been used for the central part of the potential. Magic numbers occur when there are particularly large gaps between groups of levels. Note that there is no restriction on the values of ℓ for a given *n*, unlike in the atomic case, because we do not have a Coulomb potential.

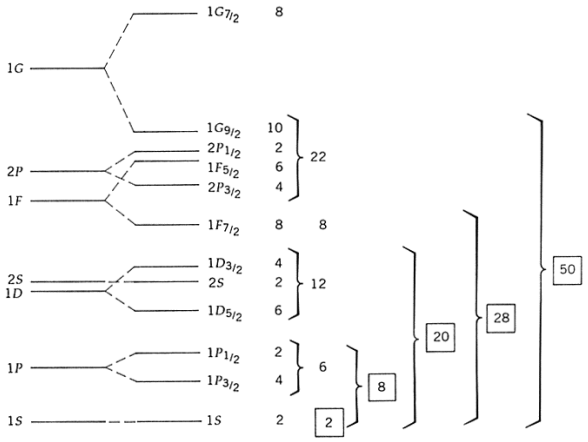

Fig.7.3 Energy levels in a single-particle shell model.
The boxed integers correspond to the magic nuclear numbers.

The *configuration* of a real nuclide (which of course has both neutrons and protons) describes the filling of its energy levels (sub-shells), for protons and for neutrons, in order, with the notation $(n\ell_j)^k$ for each sub-shell, where k is the occupancy of the given sub-shell. Sometimes, for brevity, the completely filled sub-shells are not listed, and if the highest sub-shell is nearly filled, k can be given as a negative number, indicating how far from being filled that sub-shell is. Using the ordering diagram above, and remembering that the maximum occupancy of each sub-shell is $2j+1$, we predict a configuration for $^{17}_{8}O(N=9)$ of

$$(1s_{1/2})^2(1p_{3/2})^4(1p_{1/2})^2 \qquad \text{for the protons}$$

and

$$(1s_{1/2})^2(1p_{3/2})^4(1p_{1/2})^2(1d_{5/2})^1 \qquad \text{for the neutrons}$$

Notice that all the proton sub-shells are filled, and that all the neutrons are in filled sub-shells except for the last one, which is in a sub-shell on its own. Most of the ground state properties of $^{17}_{8}O(N=9)$ can therefore be found from just stating the neutron configuration as $(1d_{5/2})^1$.

7.3 Spins, parities and magnetic moments in the shell model

The nuclear shell model can be used to make predictions about the *spins* of ground states. A filled sub-shell must have zero total angular momentum, because j is always an integer-plus-a-half, so the occupancy of the sub-shell, $2j+1$, is always an even number. This means that in a filled sub-shell, for each nucleon of a given m_j (= j_z) there is another having the opposite m_j, so that the pair have a combined m_j of zero, and so the complete sub-shell will also have zero m_j. Since this is true whatever axis we choose for z, the total angular momentum must also be zero. Since magic number nuclides have closed sub-shells, such nuclides are predicted to have zero contribution to the nuclear spin from the neutrons or protons or both, whichever are of magic number. Hence magic-*Z*/magic-*N* nuclei are predicted to have zero nuclear spin. This is indeed found to be the case experimentally.

In fact it is found that *all* even-*Z*/even-*N* nuclei have zero nuclear spin. We can therefore make the *hypothesis* that for ground state nuclei, pairs of neutrons and pairs of protons in a given sub-shell *always* couple to give a combined angular momentum of zero, even when the sub-shell is not filled. This is called the *pairing hypothesis*. We can now see why it is the last proton and/or last neutron, which determines the net nuclear spin, because these are the only ones that may not be paired up. In odd-*A* nuclides there is only one unpaired nucleon, so we can predict precisely what the nuclear spin will be by referring to the filling diagram. For even-*A* odd-*Z*/odd-*N* nuclides we will have an unpaired proton and an unpaired neutron. We cannot then make a precise prediction about the net spin because of the vectorial way that angular momenta combine; all we can say is that the nuclear spin will lie in the range $|j_p - j_n|$ to $(j_p + j_n)$.

Predictions can also be made about nuclear *parities*. Recall: (i) parity is the transformation $\mathbf{r} \to -\mathbf{r}$; (ii) the wavefunction of a single-particle quantum state will contain an angular part proportional to the spherical harmonic $Y_m^l(\theta,\phi)$, which under the parity transformation

$$P\,Y_m^l(\theta,\phi) = (-)^\ell Y_m^l(\theta,\phi)$$

Thus the parity of a single-particle quantum state depends exclusively on the orbital angular momentum quantum number with $P=(-1)^\ell$. The total parity of a multiparticle state is the *product* of the parities of the individual particles. A pair of particles with the same ℓ will therefore always have a combined parity of +1. The pairing hypothesis then tells us that the total parity of a nucleus is found from the product of the parities of the last proton and the last neutron. So we can predict the parity of *any* nuclide, including the odd/odd ones and these predictions are in agreement with experiment.

The shell model can also be used to make predictions about nuclear *magnetic (dipole) moments*. Unless the nuclear spin is zero, we expect nuclei to have magnetic moments, since both the proton and the neutron have intrinsic magnetic moments, and the proton is electrically charged, so it can produce a magnetic moment when it has orbital motion. Using a notation similar to that used in atomic physics, we can write the nuclear magnetic moment as

$$\mu = g_j\, j\, \mu_N$$

where μ_N is the *nuclear magneton* given by

$$\mu_N = e\hbar/2M_p$$

g_j is the *Landé g-factor*, j is the nuclear spin quantum number, and M_p is the proton mass. For brevity we can write simply $\mu = g_j\, j$ magnetons.

We will find that the shell model does not give very accurate predictions for magnetic moments, even for the even-odd nuclei when there is only a single unpaired nucleon in the ground state. We will not therefore consider at all the much more problematic case of the odd-odd nuclei having an unpaired proton and an unpaired neutron.

For the even-odd nuclei, we would expect all the paired nucleons to contribute no net magnetic moment, for the same reason that they do not contribute to the nuclear spin. Predicting the nuclear magnetic moment is then a matter of finding the correct way to

combine orbital and intrinsic components of magnetic moment of the single unpaired nucleon. We need to combine the spin component of the moment, $g_s s$, with the orbital component, $g_\ell \ell$ (where g_s and g_ℓ are the g-factors for spin and orbital angular momentum.) to give the total moment $g_j j$. The general formula for doing this is

$$g_j = \frac{j(j+1)+\ell(\ell+1)-s(s+1)}{2j(j+1)} g_\ell + \frac{j(j+1)-\ell(\ell+1)+s(s+1)}{2j(j+1)} g_s$$

which simplifies considerably because we always have $j = \ell \pm 1/2$. Thus

$$j g_j = g_\ell \ell + g_s/2 \quad \text{for } j = \ell + 1/2$$

$$j g_j = g_\ell j\left(1+\frac{1}{2\ell+1}\right) - g_s j\left(\frac{1}{2\ell+1}\right) \quad \text{for } j = \ell - 1/2$$

Since $g_\ell = 1$ for a proton and 0 for a neutron, and g_s is approximately +5.6 for the proton and –3.8 for the neutron, we find

$$j g_{proton} = \ell + 5.6 \times \frac{1}{2} = j + 2.8 \quad \text{for } j = \ell + 1/2$$

$$j g_{proton} = j\left(1+\frac{1}{2\ell+1}\right) - 5.6 \times j\left(\frac{1}{2\ell+1}\right) = 1 - \frac{2.3}{j+1} \quad \text{for } j = \ell - 1/2$$

$$j g_{neutron} = -3.8 \times \frac{1}{2} = -1.9 \quad \text{for } j = \ell + 1/2$$

$$j g_{neutron} = 3.8 \times j\left(\frac{1}{2\ell+1}\right) = \frac{1.9j}{j+1} \quad \text{for } j = \ell - 1/2$$

For a given j, the measured moments usually lie somewhere between the $j = \ell - 1/2$ and the $j = \ell + 1/2$ values, but beyond that, the model does not predict the moments accurately, except for nuclei with small numbers of nucleons which are close to magic values.

Why should the shell model work so well when predicting nuclear spins and parities, but be poor for magnetic moments? There are several likely problem areas, including the possibility that protons and neutrons inside nuclei may have effective intrinsic magnetic moments that are different to their free-particle values, because of their very close proximity to one another.

7.4 Excited states in the shell model

In principle, the shell model's energy level structure can be used to predict nuclear states away from the ground state, i.e. the excited states. This works quite well for the first one or two excited states when there is only one possible configuration of the nucleus. But for higher excited states the spectrum becomes very complicated because several nucleons can be excited simultaneously into a superposition of many different configurations to produce a given nuclear spin and parity.

When trying to predict the first one or two excited states using a filling diagram like Fig.7.3, we are looking for the configuration that is nearest to the ground state configuration. This will normally involve *either* moving an unpaired nucleon to the next highest level, *or* moving a nucleon from the sub-shell below the unpaired nucleon up one level to pair with it. Thus it is necessary to consider levels just above and below the last nucleons (protons and neutrons).

As an example, consider $^{17}_{8}O$, which we found to have a ground state configuration of

$$(1s_{1/2})^2 (1p_{3/2})^4 (1p_{1/2})^2 \qquad \text{for the protons}$$

and

$$(1s_{1/2})^2 (1p_{3/2})^4 (1p_{1/2})^2 (1d_{5/2})^1 \qquad \text{for the neutrons}$$

All the proton sub-shells are filled, and all the neutrons are in filled sub-shells except for the last one, which is in a sub-shell on its own. There are three possibilities to consider for the first excited state:

1. Promote one of the $1p_{1/2}$ protons to $1d_{5/2}$, giving a configuration of $(1p_{1/2})^{-1}(1d_{5/2})^1$, where the superscript –1 means that the shell is one particle short of being filled.
2. Promote one of the $1p_{1/2}$ neutrons to $1d_{5/2}$, giving a configuration of $(1p_{1/2})^{-1}(1d_{5/2})^2$.
3. Promote the $1d_{5/2}$ neutron to the next level, which is probably $2s_{1/2}$ (or the nearby $1d_{3/2}$), giving a configuration of $(1s_{1/2})^1$ or $(1d_{3/2})^1$.

Following the diagram of Fig.7.3, the third of these possibilities would correspond to the smallest energy shift, so it should be favoured over the others. The next excited state might involve moving the last neutron up a further level to $1d_{3/2}$, or putting it back where it was and adopting configurations (1) or (2). Option (2) is favoured over (1) because it keeps the excited neutron paired with another, which should have a slightly lower energy than creating two unpaired protons. When comparing these predictions with the observed excited levels it is found that the expected excited states do exist, but not necessarily in precisely the order anticipated.

The shell model has many limitations, most of which can be traced to its fundamental assumption that the nucleons move independently of one another in a spherically symmetric potential. The latter, for example, is only true for nuclei that are close to having doubly filled magnetic shells and predicts zero quadruple moments, whereas in practice nuclei are deformed and quadruple moments are often substantial.

7.5 Collective Model

The shell model is based upon the idea that the constituent parts of a nucleus move independently. The liquid drop model implies just the opposite, since in a drop of incompressible liquid, the motion of any constituent part is correlated with the motion of all the neighbouring pairs. This emphasizes that *models* in physics have a limited range of applicability and may be unsuitable if applied to a different set of phenomena. As knowledge evolves, it is natural to try and incorporate more phenomena by modifying the model to become more general, until (hopefully) we have a model with firm theoretical underpinning that describes a very wide range of phenomena, i.e. a *theory*. A step in this direction in nuclear physics is the *collective model* which uses the ideas of both the shell and liquid drop models.

The collective model assumes that the nucleons in unfilled subshells move independently in the nuclear potential produced by the core of filled subshells, as in the shell model. However, this potential is not the static, spherically symmetric potential used in the shell model, but is a potential capable of undergoing deformations in shape. These deformations represent the collective (correlated) motion of the nucleons in the core of the nucleus that are associated with the liquid drop model. I will not discuss this model further, except to say that it can

explain some properties of nuclei (e.g. electric quadruple moments) that other models cannot. A summary of the features of various nuclear models is given in Table 7.1

Table 7.1 Nuclear models and the ground state properties of nuclei

Name	Assumptions	Theory Used	Properties Predicted
Liquid drop model	Nuclei have similar mass densities, and binding energies nearly proportional to masses—like charged liquid drops	Classical (asymmetry and pairing terms introduced with no justification)	Accurate average masses and binding energies through semiempirical mass formula
Fermi gas model	Nucleons move independently in net nuclear potential	Quantum statistics of Fermi gas of nucleons	Depth of net nuclear potential Asymmetry term
Shell model	Nucleons move independently in net nuclear potential, with strong inverted spin-orbit coupling	Schroedinger equation solved for net nuclear potential	Magic numbers Nuclear spins Nuclear parities Pairing term
Collective model	Net nuclear potential undergoes deformations	Schroedinger equation solved for non-spherical net nuclear potential	Magnetic dipole moments Electric quadrupole moments

7.6 β – Decay : theory

(a) Fermi theory

The first successful theory of nuclear beta-decay was proposed in the 1930s by Fermi, long before the *W* and *Z* bosons were known and the quark model formulated. He therefore had to construct a theory based on very general principles, working by analogy with the quantum theory of electromagnetic processes (QED).

The general equation for electron β-decay is

$$ {}^{A}_{Z}X \rightarrow {}^{A}_{Z+1}Y + e^{-} + \bar{\nu}_e $$

which we have met in earlier lectures. There we interpreted this reaction as the decay of a bound neutron, i.e. $n \rightarrow p + e^{-} + \bar{\nu}_e$ and later we gave the quark interpretation of this decay. In general, it is possible for the internal state of the nucleus to change in other ways during the transition, but we will simplify matters by considering just the basic neutron decay process.

We have also met Fermi's Second Golden Rule, which enables transition rates to be calculated provided the interaction is relatively weak. (This is because it is based on perturbation theory.) We will write Fermi's Rule as

$$ \omega = \frac{2\pi}{\hbar}|M|^2 n(E) $$

where ω is the transition rate (probability per unit time), *M* is the *transition amplitude* (also

called the *matrix element* because it is one element of a matrix whose elements are all the possible transitions to different final states of the system) and $n(E)$ is the density of states, i.e. number of quantum states available to the final system per unit interval of total energy. The density-of-states factor can be calculated from purely kinematical factors, such as energies, momenta, masses, and spins where appropriate. (We did this when discussing the relationship between the scattering amplitude and cross-sections and also in the Fermi gas model) The *dynamics* of the process is contained in the matrix element.

The matrix element can in general be written in terms of one of five basic classes of Lorentz invariant interaction operators, $\mathcal{O}$:

$$ M = \int \Psi_f^* \, (g\mathcal{O}) \, \Psi_i \, \mathrm{d}V $$

where Ψ_f and Ψ_i are total wave-functions for the final and initial states, respectively, g is a dimensionless coupling constant, and the integral is over three-dimensional space (V = volume). The five categories are called *scalar* ("S"), *pseudo-scalar* ("P"), *vector* ("V"), *axial-vector* ("A"), and *tensor* ("T"), the names having their origin in the mathematical transformation properties of the operators. (We have met the *V* and *A* forms previously in Section 6 on the electroweak interaction.) The main difference between them is the effect on the spin states of the particles. When there are no spins involved, and at low energies, $(g\mathcal{O})$ is simply the interaction potential: that part of the potential that is responsible for the change of state of the system.

Fermi guessed that $\mathcal{O}$ would be of the vector type, since the electromagnetic interaction is a vector interaction, i.e. it is transmitted by a spin-1 particle – the photon. We have seen from earlier lectures that we now know that the weak interaction violates parity conservation and is correctly written as a mixture of both vector and axial-vector interactions, but so long as we are not concerned with the spins of the particles, this doesn't make much difference, and we can think of the matrix element in terms of a classical weak interaction potential, like the Yukawa potential. Applying a bit of modern insight, we can consider that the potential is of extremely short range (because of the large mass of the W boson) in which case we have seen that we can approximate the interaction by a point-like interaction and the matrix element becomes simply a constant, written as

$$ M = \frac{G_F}{V}. $$

V is the arbitrary volume, which is used to normalise the wave-functions. (It will eventually cancel out with a factor coming from the density of states term.) G_F is called the *Fermi coupling constant* and has dimensions [energy][length]^3. In nuclear theory, Fermi's coupling constant G_F is taken to be a universal constant and with appropriate corrections for changes of the nuclear state during beta decay, experimental results are consistent with the theory under this assumption. But the theory goes beyond nuclear beta decay, and can be applied to any process mediated by the W-boson — provided the energy is not too great. Thus, the best process to determine the value of G_F is one not complicated by hadronic (nuclear) effects and from purely muon decay one can deduce that the value of G_F is about $90\,\mathrm{eV\ fm^3}$. It is often quoted in the form $G_F/(\hbar c)^3 = 1.166 \times 10^{-5}\,\mathrm{GeV}^{-2}$.

(b) Electron momentum distribution

We see that the transition rate (i.e. beta-decay lifetime) depends essentially on kinematical factors arising through the density-of-states factor, $n(E)$. To simplify the evaluation of this factor, we consider the neutron and proton to be "heavy", so that they have negligible kinetic energy, and all of the energy released in the decay process goes into creating the electron and neutrino and in giving them kinetic energy. Thus we write

$$E = E_e + E_\nu$$

where E_e is the total (relativistic) energy of the electron, E_ν is the total energy of the neutrino, and E is the total energy released [$= (\Delta m)c^2$, if Δm is the neutron-proton mass difference, or the change in mass of the decaying nucleus].

The transition rate, ω, can be measured as a function of the electron momentum, so we need to obtain an expression for the spectrum of beta-decay electrons. Thus we will fix E_e and find the *differential* transition rate for decays where the electron has an energy in the range E_e to $E_e + dE_e$. From Fermi's Rule, this is

$$d\omega = \frac{2\pi}{\hbar}|M|^2 n_\nu(E - E_e) n_e(E_e)\, dE_e$$

where n_e and n_ν are the density of states factors for the electron and neutrino, respectively. These may be obtained from our previous result:

$$n(p_e)dp_e = \frac{V}{(2\pi\hbar)^3} 4\pi\, p_e{}^2 dp_e$$

with a similar expression for n_ν, by changing variables using $dp/dE = E/pc^2$, so that

$$n(E_e)dE_e = \frac{4\pi V}{(2\pi\hbar)^3 c^2}\, p_e E_e\, dE_e$$

with a similar expression for $n(E_\nu)$. Using these in the expression for $d\omega$ and setting $M = G_F/V$, gives

$$\frac{d\omega}{dE_e} = \frac{G_F{}^2}{2\pi^3\hbar^7 c^4}\, p_e E_e p_\nu E_\nu$$

where in general

$$p_\nu c = \sqrt{E_\nu^2 - m_\nu^2 c^4} = \sqrt{(E - E_e)^2 - m_\nu^2 c^4}$$

Finally, it is useful to write this as

$$\frac{d\omega}{dp_e} = \frac{dE_e}{dp_e}\frac{d\omega}{dE_e} = \frac{G_F{}^2}{2\pi^3\hbar^7 c^2}\, p_e{}^2 p_\nu E_\nu$$

If we take the antineutrino to be *precisely* massless, then $p_\nu = E_\nu/c$ and we have

$$\frac{d\omega}{dp_e} = \frac{G_F^2\, p_e^2\, p_\nu^2}{2\pi^3\hbar^7 c} = \frac{G_F^2\, p_e^2\, E_\nu^2}{2\pi^3\hbar^7 c^3} = \frac{G_F^2\, p_e^2 (E - E_e)^2}{2\pi^3\hbar^7 c^3}$$

This expression gives rise to a bell-shaped electron momentum distribution, which rises from zero at zero momentum, reaches a peak and falls to zero again at an electron energy equal to E, as illustrated in the curve labelled $Z = 0$ in Fig.7.4. Studying the precise shape of the distribution near its upper end-point is one way in principle of finding a value for the antineutrino mass. If the mass is zero mass, then the gradient of the curve approaches zero at the end-point, whereas any non-zero value results in an end-point that falls to zero with an asymptotically infinite gradient. (See Fig.7.4 – note that the insert to this figure is not accurately drawn.) We return to this below.

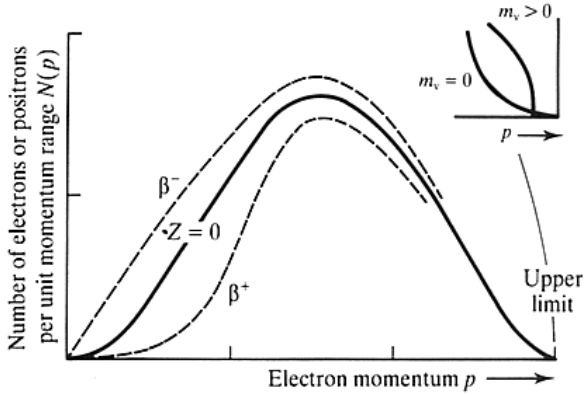

Fig.7.4 Predicted electron spectrum: $Z = 0$, without Fermi screening factor; $\beta^\pm$, spectra with Fermi screening factor

There are several factors that we have ignored or over-simplified in getting this momentum distribution. The principal ones are to do with the possible changes of nuclear spin of the decaying nucleus, and the electric force acting between the beta particle (electron or positron) and the nucleus. When the electron/antineutrino carry away a combined angular momentum of 0 or 1, the above treatment is essentially correct: these are the so-called *"allowed transitions"*. However, the nucleus may change its spin by more than 1 unit, and then the simplified short-range-potential approach to the matrix element is inaccurate. The decay rate in these cases is generally suppressed, although not completely forbidden, despite these being traditionally known as the *"forbidden transitions"*.

The electric potential between the positive nucleus and a positive beta particle will cause a shift of the low end of its momentum spectrum to the right, since it is propelled away by electrostatic repulsion. Conversely, the low end of the negative beta spectrum is shifted to the left. (See Fig.7.4.) The precise form of these effects is difficult to calculate, and requires quantum mechanics, but the results are published in tables of a factor $F(Z,E_e)$, called the *Fermi screening factor*, to be applied to the basic beta spectrum.

(c) Kurie plots and the neutrino mass

The usual way of experimentally testing the form of the electron momentum spectrum given by the Fermi theory is by means of a *Kurie plot*. From the above equations, with the Fermi

screening factor included, we have

$$\frac{\mathrm{d}\omega}{\mathrm{d}\,p_e} = \frac{F(Z,E_e)G_F^2\,p_e^2\left(E-E_e\right)^2}{2\pi^3\hbar^7c^3}$$

which we can write as

$$H(E_e) \equiv \sqrt{\left(\frac{\mathrm{d}\omega}{\mathrm{d}\,p_e}\right)\frac{1}{p_e^2K(Z,p_e)}} = E - E_e$$

where $K(Z,p_e)$ includes $F(Z,E_e)$ and all the fixed constants. A plot of the left-hand-side of this equation — using the measured $d\omega/dp_e$ and p_e and the calculated $K(Z,p_e)$ — against the electron energy E_e should then give a straight line with an intercept of E. An example is shown in Fig.7.5.

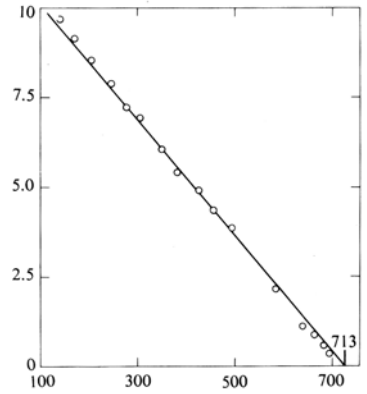

Fig.7.5 Kurie plot for the decay ^{36}Cl.
(The y-axis is proportional to the function $H(E_e)$ above.)

If the neutrino mass is not exactly zero then it is straightforward to repeat the above derivation and to show that the left-hand side of the Kurie plot is proportional to

$$\sqrt{\left(E-E_e\right)}\sqrt{\left(E-E_e\right)^2 - m_\nu{}^2c^4}$$

This will produce a *very* small deviation from linearity close to the end point of the spectrum as shown schematically in Fig.7.6. (n.b. the y-axis of this graph is actually the function $H(E_e)$ defined earlier.)

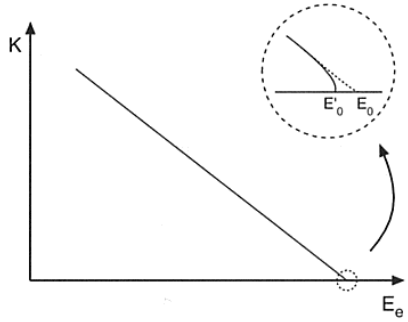

Fig.7.6 Schematic Kurie plot. If the neutrino mass is not zero, the straight line curves near the end point and cuts the axis vertically at $E_0' = E_0 - m_\nu c^2$.

In order to measure the neutrino mass to reasonable accuracy, it is necessary to use a nucleus where the non-zero mass has a maximum effect, i.e. the maximum energy release $E = E_0$ should only be a few kev. Also at low energies atomic effects have to be taken into account, so the initial and final atomic states must be very well understood. The most suitable case is the decay of tritium

$$^3H \rightarrow {}^3He + e^- + \bar{\nu}_e$$

where $E_0 = 18.6\mathrm{keV}$. Since the counting rate near E_0 is vanishingly small, the experiment is extremely difficult. In practice, the above formula is fitted to data close to the end point of the spectrum and extrapolated to E_0. The best experiments are consistent with a zero neutrino mass, but when experimental and theoretical uncertainties are taken into account, an upper limit of $3eV/c^2$ is quoted.